

**FORM FINDING AND SHAPE CHANGE
ANALYSIS OF SPINE INSPIRED
BIO-TENSEGRITY MODEL**

OH CHAI LIAN

UNIVERSITI SAINS MALAYSIA

2017

**FORM FINDING AND SHAPE CHANGE ANALYSIS OF
SPINE INSPIRED BIO-TENSEGRITY MODEL**

by

OH CHAI LIAN

**Thesis submitted in fulfillment of the
requirements for the degree of
Doctor of Philosophy**

March 2017

ACKNOWLEDGEMENTS

I would like to express my deepest gratitude to my PhD degree main supervisor, Associate Profesor Dr. Choong Kok Keong, Deputy Dean (Research), School of Civil Engineering, Universiti Sains Malaysia, Malaysia. The success of the study would not be possible without his high quality supervision, continuous guidance and supports. His dedication, patience, motivation, and immense knowledge to help his students has fruitful the study.

My special thanks also go to my co-supervisor, Profesor Dr. Toku Nishimura, Department of Architecture, Institute of Disaster and Environmental Science, Kanazawa Institute of Technology, Japan. I would not be able to understand thoroughly the formulation and programming of complex problems without his proper coach. He is keen in caring, nurturing and developing skills in his students.

Appreciation also go to external examiner Professor Mahkoto Ohsaki and internal examiners Professor Dr. Taksiah A. Majid and Associate Professor Dr. Fatimah De'nan of this thesis, for their patiece in reading and comments this thesis.

I wish to acknowledge Ministry of Higher Education and Universiti Teknologi Mara (UiTM), Malaysia for the support in PhD scholarships.

I would like to extend my appreciation to Universiti Sains Malaysia especially Scool of Civil Engineering for providing good facilities throughout my study. Their staffs are co-operative and kind to help.

Finally, I would like to thank to my family, for their loves and encouragements.

TABLE OF CONTENTS

	Page
ACKNOWLEDGMENTS	ii
TABLE OF CONTENTS	iii
LIST OF TABLES	vii
LIST OF FIGURE	viii
LIST OF ABBREVIATIONS	xiii
LIST OF SYMBOLS	xiv
ABSTRAK	xvi
ABSTRACT	xviii
CHAPTER ONE : INTRODUCTION	
1.1 Introduction	1
1.2 Tensegrity	2
1.2.1 Potential of Tensegrity for Shape Change	3
1.3 Application of Tensegrity System in Biology	7
1.4 Characteristics of Biotensegrity	10
1.4.1 Efficiency	10
1.4.2 Self Stabilization	11
1.4.3 Multi-Modularity	12
1.4.4 Multi-Functional	12
1.5 Motivation from Spine Biotensegrity	13
1.6 Problem Statement	15
1.7 Objectives	18
1.8 Scope of Work	18
1.9 Layout of Thesis	19

CHAPTER TWO : LITERATURE REVIEW

2.1	Introduction	20
2.2	Biotensegrity in Anatomy and Physiology	22
2.2.1	Anatomy	22
2.2.2	Physiology	24
2.3	Cellular Biotensegrity	27
2.3.1	Configuration of Cellular Tensegrity	28
2.3.2	Elementary Functions of Cellular Tensegrity	29
2.3.3	Mechanical Properties of Cellular Tensegrity	31
2.4	Potential Applications of Biotensegrity	35
2.5	Summary	38

CHAPTER THREE : METHODOLOGY

3.1	Description of Tensegrity Mast	40
3.2	Geometrical Inputs from Human Spine	42
3.2.1	Vertebrae Anatomical Parameters	42
3.2.2	Natural Sagittal Curvature	43
3.3	Search Strategies for SBS Model	46
3.3.1	Generation of SBS Model	46
3.3.2	Formulation of Equations for Self-Equilibrated State of SBS Model	52
3.3.3	Algorithm for Form Finding of SBS Model	58
3.4	Computational Strategies for Shape Change Analysis of SBS Model	61
3.4.1	Derivation of Incremental Equilibrium Equations for SBS Model	61
3.4.2	Optimization of Forced Elongation by SQP	68
3.4.3	Proposed Algorithm for Shape Change for SBS Model	73
3.5	Target Displacements in Shape Change Analysis	77
3.5.1	Cases of Target Displacements in Uni-Directional Mode	77

3.5.2	Cases of Target Displacements in Bi-Directional Mode	78
3.5.3	Cases of Target Displacements in Tri-Directional Mode	79
3.5.4	Cases of Target Displacements in Twisting Mode	80
3.6	Examination of Structural Characteristics of SBS Models	81

CHAPTER FOUR : RESULTS AND DICUSSION

4.1	Configuration Search Results for SBS Models	82
4.1.1	Initial Topology of Four-Stage SBS Models	82
4.1.2	Optimization of Coefficient β	85
4.1.3	Effects of Twisting Angles on Slackened Cables	85
4.1.4	Effect of Modified Nodal Coordinates on Slackened Cables	89
4.1.5	Findings from the Searched of Novel SBS Models	102
4.2	Performance of Proposed Algorithm for Shape Change Analysis	104
4.2.1	Application on Numerical Examples of Tensegrity Models	104
4.2.2	Numerical Application on SBS Model	119
4.2.3	Displacements of Monitored Nodes	139
4.2.4	Evaluation on Convergence of Algorithm of Shape Change Analysis	156
4.3	Structural Characteristics of SBS Models	158
4.3.1	Deformation Modes	158
4.3.2	Changes in Axial Forces	186
4.3.3	Evaluation on Characteristics of Deformed State of SBS Models	211

CHAPTER FIVE : CONCLUSIONS

5.1	Conclusions	213
5.1.1	Configuration Search for SBS Models	213
5.1.2	Shape Change Analysis of SBS Models	214
5.1.3	Structural Characteristics of SBS Models	215

5.2 Future Works	216
------------------	-----

REFERENCES	217
-------------------	-----

APPENDICES

APPENDIX A	History of Tensegrity System
APPENDIX B	Anatomical Data for Spine Biotensegrity Models
APPENDIX C	Initial Topology of Four-stage SBS Models
APPENDIX D	Search of Self-Equilibrating SBS Models
APPENDIX E	Geometrical Inputs, Material Properties and Coefficient β for the Four Tensegrity Models
APPENDIX F	Deformation modes of SBS Models

LIST OF TABLES

		Page
Table 2.1	Summary of biotensegrity in living organisms	26
Table 3.1	Four states in shape change analysis	62
Table 4.1	Grouping of elements in SBS model and their connectivity	84
Table 4.2	Axial forces and potential twist angle for slackened cables	89
Table 4.3	Effect of modification of each nodal coordinate on axial forces of slackened cables in SB1	91
Table 4.4	Cases for modification of nodal coordinates in y direction (mm) for SB1	92
Table 4.5	Effect of modification of nodal coordinates on axial forces of slackened cables in SB1	92
Table 4.6	Effect of modification of each nodal coordinate on axial forces of slackened cables in SB2	94
Table 4.7	Effect of modification of nodal coordinates on axial forces of slackened cables in SB2	94
Table 4.8	Effect of modification of each nodal coordinate on axial forces of slackened cables in SB3	96
Table 4.9	Cases on modification of nodal coordinates in y direction (mm) for SB3	97
Table 4.10	Effect of modification of nodal coordinate on axial forces of slackened cables in SB3	97
Table 4.11	Nodal Coordinates for the searched self-equilibrated SB1, SB2 and SB3	98
Table 4.12	Total computational step in cases of Z_p , Z_n and Y_p	106
Table 4.13	Total computational step for cases with target displacements in uni-directional mode	120
Table 4.14	Total computational step for cases with target displacements in bi-directional mode	120
Table 4.15	Total computational step for cases with target displacements in tri-directional mode	123
Table 4.16	Computation steps for cases with target displacements in twisting mode	124
Table 4.17	Elements frequently in high PCF	207

LIST OF FIGURES

		Page
Figure 1.1	Three-strut tensegrity structure	2
Figure 1.2	Deployable tensegrity structures	4
Figure 1.3	Tensegrity robots	6
Figure 1.4	Tetraspine prototype	7
Figure 1.5	Examples of biotensegrity	9
Figure 1.6	Characteristics of spine biotensegrity	14
Figure 1.7	Spiral vertebra mast and Icosahedral chain	15
Figure 1.8	Motivation for the study	17
Figure 2.1	Examples of cellular tensegrity model	33
Figure 3.1	Triangular cell	41
Figure 3.2	Two-stage tensegrity mast	41
Figure 3.3	Typical vertebra parameters	42
Figure 3.4	Human spine anatomy lateral and posterior view	44
Figure 3.5	Construction of curvature line mimicking human spine	45
Figure 3.6	Definition for typical triangular prism and triangular surfaces for SBS models	47
Figure 3.7	Element connectivity of N-stage class 1 three-strut SBS model	49
Figure 3.8	Assemblage of SBS model	51
Figure 3.9	A three-dimensional pinned jointed SBS element	53
Figure 3.10	Modification of current nodal coordinate	59
Figure 3.11	Algorithm for form finding of SBS model	60
Figure 3.12	Configuration of element k of SBS model during shape change analysis	63
Figure 3.13	Length of element k at initial state, deformed state and shape change state	64
Figure 3.14	Terminology of nodal coordinates of monitored nodes during the shape change analysis	68

Figure 3.15	Example of B_1	70
Figure 3.16	Algorithm for shape change analysis	76
Figure 3.17	Cases of target displacements in uni-directional mode	78
Figure 3.18	Cases of target displacements in bi-directional mode	79
Figure 3.19	Cases of target displacements in tri-directional mode	80
Figure 3.20	Cases of target displacements in twisting mode	81
Figure 4.1	Positions and dimensions of triangular surfaces in SB1, SB2 and SB3	83
Figure 4.2	Effect of overall twisting angles on number of slackened cables	86
Figure 4.3	Effect of varies combination of twist angles on number of slackened cables for SB1	87
Figure 4.4	Effect of various twist angles for triangular cell at stage 1 on number of slackened cables in SB1, SB2 and SB3	88
Figure 4.5	Self-equilibrated configuration for SB1	99
Figure 4.6	Self-equilibrated configuration for SB2	100
Figure 4.7	Self-equilibrated configuration for SB3	101
Figure 4.8	Types of studied tensegrity models	105
Figure 4.9	Normalized objective function plot for cases of Z_p , Z_n and Y_p	107
Figure 4.10	Shape change of simplex for case Z_p	109
Figure 4.11	Shape change of quadruplex for case Z_p	109
Figure 4.12	Plan view of (a) simplex and (b) quadruplex, for case Z_p	110
Figure 4.13	Shape change of two-stage tensegrity model for case Z_p	111
Figure 4.14	Shape change of tapered three-stage tensegrity model for case Z_p	111
Figure 4.15	Shape change of simplex for case Z_n	113
Figure 4.16	Shape change of quadruplex for case Z_n	113
Figure 4.17	Plan view of (a) simplex and (b) quadruplex, for case Z_n	114
Figure 4.18	Shape change of two-stage tensegrity model for case Z_n	114
Figure 4.19	Shape change of tapered three-stage tensegrity model for case Z_n	115
Figure 4.20	Shape change of simplex for case Y_p	117

Figure 4.21	Shape change of quadruplex for case Yp	117
Figure 4.22	Shape change of two-stage tensegrity model for case Yp	118
Figure 4.23	Shape change of tapered three-stage tensegrity model for case Yp	118
Figure 4.24	Normalized objective function for cases of uni-directional mode	126
Figure 4.25	Normalized objective function for cases of bi-directional mode	129
Figure 4.26	Normalized objective function for cases of tri-directional mode (series XY200)	132
Figure 4.27	Normalized objective function for cases of tri-directional mode (series XY400)	134
Figure 4.28	Normalized objective function for twisting mode series	137
Figure 4.29	Displacement of monitored nodes of cases with target coordinate in uni-directional mode	140
Figure 4.30	Displacement of monitored nodes of cases with target coordinate in bi-directional mode	143
Figure 4.31	Displacement of monitored nodes of cases with target coordinate in tri-directional mode for series XY200Z and XY400Z	146
Figure 4.32	Displacement of monitored nodes of cases with target coordinate in tri-directional mode of series XY200Zp	147
Figure 4.33	Displacement of monitored nodes of cases with target coordinate in tri-directional mode of series XY200Zn	148
Figure 4.34	Displacement of monitored nodes of cases with target coordinate in tri-directional mode of series XY400Zp	150
Figure 4.35	Displacement of monitored nodes of cases with target coordinate in tri-directional mode of series XY400Zn	151
Figure 4.36	Displacement of monitored nodes of with target coordinate in twisting mode series Z	153
Figure 4.37	Displacement of monitored nodes of with target coordinate in twisting mode series Zp	154
Figure 4.38	Displacements of monitored nodes of with target coordinate in twisting mode Series Zn	155
Figure 4.39	Deformed configuration (a) at step 1 and (b-f) at final step for series Xn and Xp	160
Figure 4.40	Deformed configuration (a) at step 1 and (b-f) at final step for series Yn and Yp	161

Figure 4.41	Deformed configuration (a) at step 1 and (b-f) at final step for series Zn	162
Figure 4.42	Deformed configuration (a) at step 1 and (b-d) at final step for series Zp	164
Figure 4.43	Deformed configuration (a) at step 1 and (b-f) at final step for cases with bi-directional mode (target displacement magnitude 200mm)	167
Figure 4.44	Deformed configuration (a) at step 1 and (b-f) at final step for cases with bi-directional mode (target displacement magnitude 400mm)	168
Figure 4.45	Deformed configuration (a) at step 1 and (b-f) at final step for cases with bi-directional mode (target displacement magnitude 600mm)	169
Figure 4.46	Deformed configuration (a) at step 1 and (b-f) at final step for cases with tri-directional mode (Series XY200Z and XY400Z)	171
Figure 4.47	Deformed configuration (a) at step 1 and (b-d) at final step for cases with tri-directional mode (Series XY200Zp)	173
Figure 4.48	Deformed configuration (a) at step 1 and (b-d) at final step for cases with tri-Directional mode (Series XY400Zp)	174
Figure 4.49	Deformed configuration (a) at step 1 and (b-d) at final step for cases with tri-directional mode (Cases of XY200Zn200)	176
Figure 4.50	Deformed configuration (a) at step 1 and (b-d) at final step for cases with tri-directional mode (Cases of XY200Zn400)	177
Figure 4.51	Deformed configuration (a) at step 1 and (b-d) at final step for cases with tri-directional mode (Case of XY200Zn600)	178
Figure 4.52	Deformed configuration (a) at step 1 and (b-d) at final step for cases with tri-directional (Series XY400Zn)	179
Figure 4.53	Deformed configuration (a) at step 1 and (b-e) at final step for analysis case SB3Tor90Z	181
Figure 4.54	Deformed configuration (a) at step 1 and (b-e) at final step for analysis case SB2Tor150Z	182
Figure 4.55	Deformed configuration (a) at step 1 and (b-f) at final step for series with twisting mode (Series Zp)	184
Figure 4.56	Deformed configuration (a) at step 1 and (b-f) at final step for series with twisting mode (Series Zn)	185
Figure 4.57	Axial Forces (N) at first (black) and final (white) step for series Xn	188
Figure 4.58	Axial Forces (N) at first (black) and final (white) step for series Xp	189
Figure 4.59	Axial Forces (N) at first (black) and final (white) step for series Yn	190
Figure 4.60	Axial Forces (N) at first (black) and final (white) step for series Yp	191

Figure 4.61	Axial Forces (N) at first (black) and final (white) step for series Zn	192
Figure 4.62	Axial Forces (N) at first (black) and final (white) step for series Zp	193
Figure 4.63	Axial forces (N) at first (black) and final (white) step for series XpYp	195
Figure 4.64	Axial forces (N) at first (black) and final (white) step for series XnYn	196
Figure 4.65	Axial Forces (N) at first (black) and final (white) step for series XY200Z	198
Figure 4.66	Axial Forces (N) at first (black) and final (white) step for series XpYn400Z	199
Figure 4.67	Axial Forces (N) at initial (black) and final (white) step for series XY200Zp	201
Figure 4.68	Axial Forces (N) at initial (black) and final (white) step for series XY400Zp	202
Figure 4.69	Axial Forces (N) at first (black) and final (white) step for series XY200Zn	204
Figure 4.70	Axial Forces (N) at first (black) and final (white) step for series XY400Zn	205
Figure 4.71	Axial Forces (N) at first (black) and final (white) step for series Z in cases with target displacement in twisting mode	208
Figure 4.72	Axial Forces (N) at first (black) and final (white) step for series Zp in cases with target displacement in twisting mode	209
Figure 4.73	Axial Forces (N) at first (black) and final (white) step for series Zn in cases with target displacement in twisting mode	210

LIST OF ABBREVIATIONS

SBS	Spine biotensegrity structure
EPW	Vertebral end-plate width
UEPW	Upper vertebral end-plate width
LEPW	Lower vertebral end-plate width
VBHC	Vertebral central body height
IDH	Intervertebral disc height
EPD	End-plate depth
C1	Vertebra Atlas
C2	Vertebra Axis
C3-C7	Vertebrae at Cervical region
T1-T12	Vertebrae at Thoracic region
L1-L5	Vertebrae at Lumbar region
S1-S5	Vertebrae at Sacrum region
Xn	Analysis case with target displacement in negative x direction
Yn	Analysis case with target displacement in negative y direction
Zn	Analysis case with target displacement in negative z direction
Xp	Analysis case with target displacement in positive x direction
Yp	Analysis case with target displacement in positive y direction
Zp	Analysis case with target displacement in positive z direction

LIST OF SYMBOLS

α	Twist angle
α'	Updated twist angle
h	Saddle height
\mathbf{X}	Vector of nodal coordinates
\mathbf{x}_i	Nodal coordinate vectors
L_{TK}	Total length of an element
λ	Directional cosines
\mathbf{n}	Axial force vector
n_L	Lower axial force limit
n_U	Upper axial force limit
\mathbf{f}	External force vector
m	Number of elements
n	Number of nodes
n_c	Number of constraints
n_u	Number of unconstrained degree of freedom
β	Coefficient of linearly independent vectors
\mathbf{g}	Linearly independent vectors
q	Numbers of linearly independent vectors
E	Young modulus
I	Moment of inertia
σ	Yield stress
A	Cross sectional area
k	Element k
L_0	Original length of element k
l	Length after imposition of forced elongation

u	Elastic elongation
ε	Engineering strain
\dot{u}	Length increment due to elastic elongation
\dot{l}	Forced elongation
\dot{n}	Incremental axial force
\dot{x}	Incremental nodal coordinate
\dot{x}'	Incremental nodal coordinates for specified monitored nodes
\bar{x}	Target coordinate
\mathbf{K}	Tangent stiffness matrix
\mathbf{K}_e	Linear stiffness matrix
\mathbf{K}_g	Geometrical stiffness matrix
\mathbf{H}	Hessian matrix
d_{cl}	Limit of forced elongation

PENCARIAN KONFIGURASI DAN ANALISIS PERUBAHAN BENTUK MODEL BIO-TENSEGRITY YANG DIILHAMKAN OLEH TULANG BELAKANG

ABSTRAK

Biotensegrity yang diilhamkan oleh organisma hidup memiliki sebahagian besar sifat mekanik cemerlang yang terkandung dalam sistem biologi seperti kecekapan, berkestabilan diri, berhierarki dan berupaya menyalurkan pelbagai fungsi. Di samping itu, *biotensegrity* sebagai satu model yang terhasil daripada inspirasi rupa bentuk dan fungsi sistem biologi yang berhierarki juga menunjukkan potensinya dalam perubahan bentuk. Maka, kajian *biotensegrity* sebagai satu alternatif baru dalam aplikasi yang memerlukan perubahan bentuk seperti lengan fleksibel dalam industri pembinaan adalah diperlukan. Walau bagaimanapun, penyelidikan dalam menghasilkan konfigurasi dan model matematik *biotensegrity* yang melibatkan perubahan bentuk adalah terhad. Dengan ini, model yang berinspirasi sistem biologi terutamanya dari segi rupa bentuk seperti dimensi dan lengkungan semula jadi tetulang belakang manusia yang berkeupayaan dalam perubahan bentuk untuk kegunaan sebagai alatan robot adalah tujuan utama kajian ini. Khususnya, penyelidikan ini bertujuan untuk (1) memperolehi konfigurasi model *biotensegrity* berunsurkan tetulang belakang manusia, *spine biotensegrity structure* (SBS) melalui fomulasi matematik, (2) mencadangkan algoritma untuk tujuan simulasi perubahan bentuk, dan (3) mengkaji perilaku model asli SBS. Metodologi kajian ini melibatkan tiga fasa. Dalam fasa pertama, prosedur pencarian konfigurasi model *biotensegrity* yang berunsurkan tetulang belakang manusia yang bertingkat empat dan jenis kelas satu telah diterbitkan. Usaha pencarian konfigurasi ini melibatkan kaedah menyelesaikan persamaan sistem keseimbangan melalui cara *Moore-Penrose generalized inverse*, penentuan ragam tegasan keseimbangan-diri melalui asas penguraian serta pengoptimuman pekali untuk gabungan linear ragam tegasan keseimbangan-diri. Kelebihan ciri tetulang belakang manusia seperti kelangsingan, kelengkungan semula jadi dan unsur rangkaian penstabilan seperti tetulang dan otot telah digunakan dalam pencarian konfigurasi model SBS. Di samping itu, dua kaedah khusus yang berkesan telah

digunakan dalam pencarian konfigurasi model SBS yang berkeseimbangan-diri, iaitu dengan melalui pelarasan sudut putaran dan juga penganjakan kordinasi nod asal. Setelah usaha pencarian konfigurasi model SBS yang berkeseimbangan-diri, keupayaan model tersebut menjalani proses perubahan bentuk secara tambahan telah disiasat dalam fasa kedua. Khususnya, nod model SBS yang tidak dikekang telah dipilih sebagai nod dipantau di mana nod tersebut diperlukan untuk mencapai anjakan sasaran yang dinyatakan dalam magnitud tertentu. Keupayaan dalam perubahan bentuk model SBS ke arah sasaran boleh dicapai dengan pemanjangan kabel. Strategi pengiraan untuk perubahan bentuk melibatkan dua peringkat: penerbitan persamaan keseimbangan tambahan dan pengoptimuman pemanjangan kabel dengan pengaturcaraan berjujukan quadratik (*sequential quadratic programming*). Dalam fasa ketiga, ciri-ciri model SBS seperti konfigurasi dan perubahan dalam daya paksi setelah analisis perubahan bentuk telah disiasat. Empat mod pergerakan berikut telah dikaji untuk menyiasat ciri-ciri model SBS setelah perubahan bentuk: mod pergerakan dalam satu, dua, tiga arah dan mod putaran. Kajian ini telah berjaya memperolehi konfigurasi *biotensegrity* berunsurkan tetulang belakang manusia berkeseimbangan-diri. Sebanyak tiga konfigurasi model yang baru telah dihasilkan. Kajian ini juga mencadangkan prosedur yang melibatkan pengiraan perubahan bentuk secara tambahan untuk model SBS. Simulasi berangka ke atas *tensegrity* biasa dan model SBS telah menunjukkan sifat penumpuan yang unggul untuk algoritma yang dicadangkan dalam analisis perubahan bentuk. Hasil kajian ini menunjukkan algoritma yang dicadangkan adalah berkesan bagi model yang berkeseimbangan-diri untuk mencari kordinat sasaran dalam pelbagai mod pergerakan melalui pemanjangan kabel. Hasil kajian ini juga menunjukkan bahawa model SBS berkeupayaan dalam perubahan bentuk secara lenturan, ubah bentuk paksi dan kilasan di samping menunjukkan perubahan daya dalam anggota yang ketara semasa perubahan bentuk. Perubahan daya paksi yang aktif terutama dalam kumpulan elemen yang jauh dari nod dipantau juga dikesan. Sebagai kesimpulan, hasil kajian ini memberi sumbangan ke arah merealisasikan lengan fleksibel yang berunsurkan tetulang belakang yang berkeupayaan pelbagai corak perubahan bentuk.

FORM FINDING AND SHAPE CHANGE ANALYSIS OF SPINE INSPIRED BIO-TENSEGRITY MODEL

ABSTRACT

Biotensegrity mimicking the living organisms possesses excellent characteristics that duly demonstrate most of the properties in biological systems such as efficiency, self-stabilization, multi-modularity and multi-functional. Moreover, biotensegrity as a model emulated from the forms and functions of hierarchical biological system reveals its great potential in shape change ability. Therefore it is highly suitable to study biotensegrity as a new alternative choice for possible application where shape change ability is desired such as flexible arm in construction industry. However, there are limited studies on form finding of biotensegrity configurations and mathematical models on shape change of biotensegrity. Mimicking biological system by their shape, pertinent anatomical dimensions and natural curvature of human spine to seek its potential in shape change beneficial to application like automated robotic tools is the overall aim of this study. Specifically, this basic study aims to (1) formulate mathematical procedures for finding self-equilibrated configurations of spine biotensegrity structure (SBS) models (2) formulate computational strategy for simulating the shape change of novel SBS models, and (3) evaluate the characteristics of the novel SBS models. The methodology for this study consists of three phases. In the first phase, assemblage and mathematical formulation procedure for form finding of self-equilibrated four-stage class 1 biotensegrity models inspired by human spine or spine biotensegrity (SBS) models are established. The form-finding procedure involves method of solving the system of equilibrium equations through the use of Moore-Penrose generalized inverse, determination of self-equilibrium stress modes via eigenvector basis decomposition and optimization of coefficients for the linear combination of linearly independent self-equilibrium stress modes. Advantageous features of human spine like the slenderness and natural curvature in the geometry, as well as the stabilizing network consist of spinal column and muscle are incorporated in the mathematical formulation of the configuration of the SBS

models. Additionally, two specific approaches in modification of nodal coordinates are implemented to improve the efficiency for form-finding of self-equilibrated SBS models, i.e. by means of adjustment of twist angles and modification of initial nodal coordinates. After successful searching of the configuration of self-equilibrated SBS models, the ability of the models to undergo shape change to achieve the prescribed state is investigated in the second phase. Specifically, unconstrained nodes of SBS model are chosen as monitored nodes where these nodes are required to reach a set of target displacements in prescribed magnitudes and directional modes. The shape change of SBS models towards target state is achieved by means of forced elongation of cable. Computational strategies for the shape change consist of two stages: the derivation of incremental equilibrium equations and optimization of the cables forced elongation by sequential quadratic programming. In the third phase, the structural characteristics of SBS models such as the deformed configurations and changes of axial force at the end of shape change analysis are investigated. The following four cases of target displacements are studied in order to investigate the characteristics of SBS models after shape change: uni-, bi-, tri-directional and twisting modes. The current study has successfully formulated mathematically the self-equilibrated configuration of SBS models inspired by human spine. A total of three novel self-equilibrated configurations of SBS models were searched. This study has also proposed a set of procedures involving incremental calculation for shape change analysis of SBS models. Numerical simulations of the regular tensegrity and SBS models have proven the superior convergent characteristic of the proposed algorithm for shape change analysis. The results reveal that the proposed approach for shape change analysis has a very strong ability for a self-equilibrated model to search their desired target coordinates in multi-directional modes through optimization of the forced elongation in cables. It is also found that the SBS models are capable to undergo bending, axial and torsional deformation. Active changes in forces in element groups even within the far-away element groups of SBS models are observed during the shape change analysis. In conclusion, the findings of this basic study have paved the way for realization of spine inspired flexible arm with magnitude shape change ability.

CHAPTER ONE

INTRODUCTION

1.1 Introduction

Over the past decade, extensive investigations on shape change of tensegrity structure particularly in deployable tensegrity structures and tensegrity-robots have been performed, owing to the advantageous characteristics of the tensegrity structure of being lightweight, flexible, scalability and energy efficient (Duffy et al., 2000, Korkmaz et al., 2011, Moored et al., 2011a, Koizumi et al., 2012). Stability of tensegrity structure is maintained through the integration of only compression and tensional forces through strut and cable like elements. There is a potential to convert local pressure into global deformation and subsequently seek for another balanced configuration in tensegrity. This makes tensegrity a suitable model for shape change studies. Living organisms, from as small as cells to as complete as organisms, respond to the environment in expansion and contraction to generate complex transformation for performing various functions required. The expansion and contraction mechanism in living organism has been described as biotensegrity by Levin (2002). Biotensegrity as a model emulated from the forms and functions of sophisticated and sustainable biological system is highly suitable for consideration as a new alternative choice to be adopted for robotic tools (i.e. for inspection, automation in manufacturing ect.) and deployable structures.

This chapter firstly introduces the concept of tensegrity and its shape change potential in deployable structures and robots. Next, application of tensegrity in biology or biotensegrity is introduced. The characteristics of biotensegrity are also explained based on the forms and functions of biological system. Later, motivation of spine biotensegrity model for the study is explained which is then followed by the presentation of the problem statement of the study. After the problem statement, the objectives of the study and layout of the thesis are described.

1.2 Tensegrity

Tensegrity is an amazing system with characteristics of being lightweight, self-stressed, flexible and controllable. The design of tensegrity system is different from the traditional ways with continuous transmission of compression. In tensegrity system (Figure 1.1), the tensional network is assembled in order to support the floated compression. Most importantly, the system can maintain its shape via self-equilibrium without any supports with gravitational load.

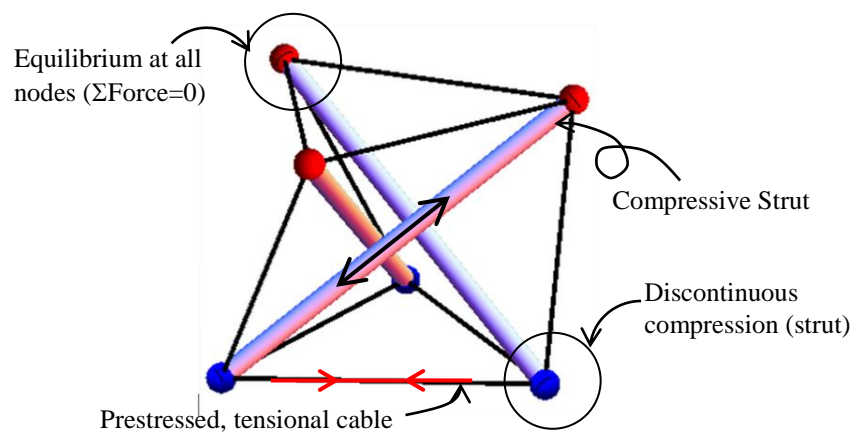


Figure 1.1 Three-strut tensegrity structure

In addition to stability, this kind of network arrangement provides aesthetics feature to the system due to its appearance of lightweightness. Although the study on tensegrity system only started since 1950's, the development and extensiveness of the study has fruitfully contributed to new independent branches of studies.

There are numbers of published definition to describe tensegrity system (Tensegritywiki, 2010a). In this study, the definition extended by Motro (2003) is adopted. According to Motro (2003), a tensegrity system is *a system in a stable self-equilibrated state comprising a discontinuous set of compressed components inside a continuum of tensioned components*. Undoubtedly, the purely compressed components at the condition of not touching each others are held in position by the continuous purely tensioned components that eventually

form tensegrity system. In the definition, the term “*system*” includes all the structures that have the qualitative or quantitative characteristics whereas term “*component*” includes wider shape of the constituent in a tensegrity system such as a line, surface, volume or combination of them. Besides, expression “*in a stable self-equilibrated state*” indicates that tensegrity systems are stable and in self-equilibrium condition. Appendix A shows the history and some patented figures of tensegrity.

1.2.1 Potential of Tensegrity for Shape Change

Deployable and transformation capability of tensegrity system has been utilized in smart, active deployable structure (particularly for space engineering) as well as the robotic and automation community in the recent years. This section surveys the shape change potential of tensegrity system especially deployable tensegrity system and tensegrity robots.

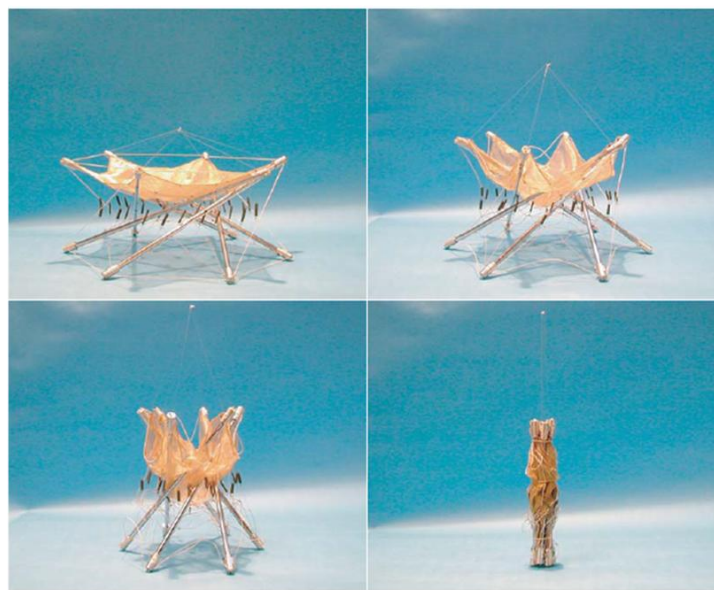
1.2.1(a) Deployable Tensegrity System

Tensegrity systems can simply alter their configuration and deal with large displacement once being loaded. Additionally, simple joints (pinned jointed) and controllable cables in tensegrity systems make them fit for use as deployable structures compared with the usage of complex joints and telescopic struts in traditional systems. Moreover, the ability of cables in tensegrity systems to act as actuator or sensor is advantageous to the design of deployable structures.

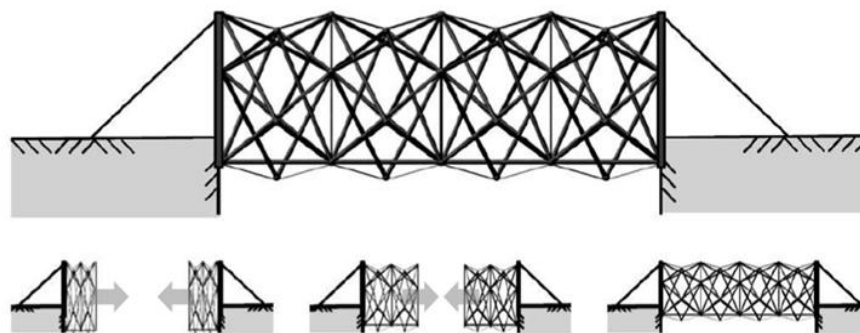
Furuya (1992) was probably the first researcher to use tensegrity as deployable structures. However the investigation was at conceptual level. A proper deployment procedure begun with the concept of cable control by Sultan and Skelton (1998). Later, a procedure was established based on cable control through symmetrical motion by Sultan et al. (2002). The deployment strategy to achieve the trajectory based on an equilibrium manifold was also presented by Sultan and Skelton (2003). Although this strategy produces widely reconfiguration shapes, control of all the cables remains the challenging issue. An

optimization method to determine the reference trajectory for deployment of an arbitrary tensegrity structure was developed by van de Wijdeven and de Jager (2005). Furthermore, a two-phase setting procedure to deploy a tensegrity beam designed under ultimate and serviceability limit state was proposed by Averseng and Dubé (2012).

Application of deployable tensegrity in ring shape as reflectors for small satellites (Figure 1.2a) was suggested by Tibert and Pellegrino (2002). The tensegrity reflector has lower construction cost and higher precision in geometrical assemblage. A deployable class 2 tensegrity boom via open loop control strategy was designed and built by Pinaud et al. (2004).



(a) Tensegrity reflector (Tibert and Pellegrino, 2002)



(b) Pentagonal tensegrity-ring footbridge (Rhode-Barbarigos et al., 2012)

Figure 1.2 Deployable tensegrity structures